Results on hyperon production from NA57

Presented by K Fanebust[i] for the NA57 collaboration:

F Antinori[a], A Badalà[b], R Barbera[b], A Belogianni[c], A Bhasin[d]‡, I J Bloodworth[d], G Bruno[e], S A Bull[d], R Caliandro[e], M Campbell[f], W Carena[f], N Carrer[f a], R F Clarke[d], A Dainese[a], A P de Haas[g], P de Rijke[g], D Di Bari[e], S Di Liberto[h], R Divia[f], D Elia[e], D Evans[d], K Fanebust[i], F Fayazzadeh[j], J Fedorišin[k], G A Feofilov[l], R A Fini[e], J Ftáčnik[m], B Ghidini[e], G Grella[n], H Helstrup[i], M Henriquez[j], A K Holme[j], A Jacholkowski[e f], G T Jones[d], P Jovanovic[d], A Jusko[o], R Kamermans[g], J B Kinson[d], K Knudson[f], A A Kolojvari[l], V Kondratiev[l], I Králik[o], A Kravcakova[k], P Kuijer[g], V Lenti[e], R Lietava[m], G Løvhøiden[j], M Lupták[o], V Manzari[e], G Martinská[k], M A Mazzoni[h], F Meddi[h], A Michalon[p], M Morando[a], D Muigg[g], E Nappi[e], F Navach[e], P I Norman[d], A Palmeri[b], G S Pappalardo[b], B Pastirčák[o], J Pišút[m], N Pišútová[m], F Posa[e], E Quercigh[f a], F Riggi[b], D Röhrich[q], G Romano[n], K Šafařík[f], L Šándor[o], E Schillings[g], G Segato[a], M Sené[r], R Sené[r], W Snoeys[f], F Soramel[a], M Spyropoulou-Stassinaki[c], P Staroba[s], T A Tulina[l], R Turrisi[a], T S Tveter[j], J Urbán[o], F F Valiev[l], A van den Brink[g], P van de Ven[g], P Vande Vyvre[f], N van Eijndhoven[g], J van Hunen[f], A Vascotto[f], T Vik[j], O Villalobos Baillie[d], L Vinogradov[l], T Virgili[n], M F Votruba[d], J Vrláková[k] and P Závada[s]

[a] Dipartimento di Fisica dell'Università and Sezione INFN, Padua, Italy
[b] Dipartimento di Fisica dell'Università and Sezione INFN, Catania, Italy
[c] Physics Department, University of Athens, Athens, Greece
[d] School of Physics and Astronomy, University of Birmingham, Birmingham, UK
[e] Dipartimento I.A. di Fisica dell'Università e del Politecnico di Bari and Sezione INFN, Bari, Italy
[f] CERN, European Laboratory for Particle Physics, Geneva, Switzerland
[g] Utrecht University and NIKHEF, Utrecht, The Netherlands
[h] Dipartimento di Fisica dell'Università "La Sapienza" and Sezione INFN, Rome,Italy
[i] Høgskolen i Bergen, Bergen, Norway
[j] Fysisk institutt, Universitetet i Oslo, Oslo, Norway
[k] P.J. Šafárik University, Košice, Slovakia
[l] State University of St. Petersburg, St. Petersburg, Russia
[m] Comenius University, Bratislava, Slovakia
[n] Dipartimento di Scienze Fisiche "E.R. Caianiello" dell'Università and INFN, Salerno, Italy
[o] Institute of Experimental Physics, Slovak Academy of Science, Košice, Slovakia
[p] Institut de Recherches Subatomiques, IN2P3/ULP, Strasbourg, France
[q] Fysisk institutt, Universitetet i Bergen, Bergen, Norway
[r] Collège de France and IN2P3, Paris, France
[s] Institute of Physics, Academy of Sciences of the Czech Republic, Prague, Czech Republic

Abstract.

The NA57 experiment has been designed to study the onset of enhanced production of strange baryons and anti-baryons in Pb-Pb collisions with respect to p-Be collisions. Results from 40 and 160 A GeV/c Pb-Pb data will be shown. The main focus is on the checks of the NA57 analysis chain.

‡ Commonwealth Fellow from Physics Department, University of Jammu, India.

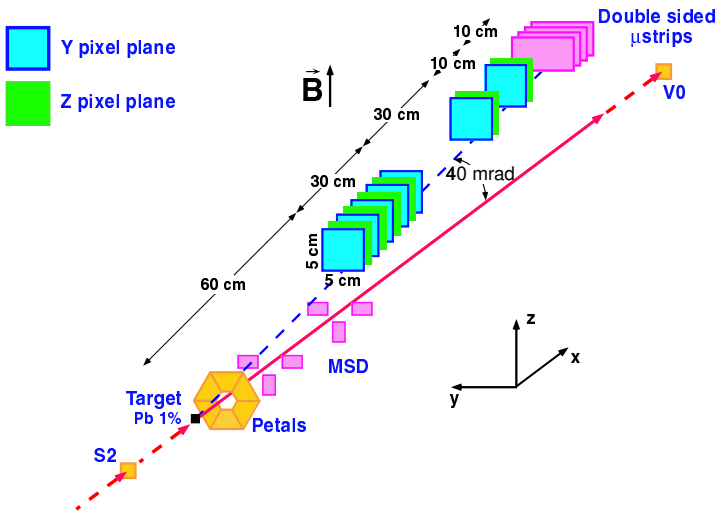

Figure 1. The NA57 experimental layout (160 A GeV/c Pb-Pb setup).

1. Introduction

The NA57 experiment continues and extends the measurements of our predecessor experiment WA97, which observed that the production of strange baryons and anti-baryons relative to non-strange particles in Pb-Pb collisions at 160 A GeV/c is enhanced with respect to p-Be collisions at the same beam momentum [1]. The enhancement increases with the strangeness content of the baryon. This behaviour has been predicted as a consequence of the QGP phase transition [2].

The NA57 experiment has been designed to look for the onset of the strange particle enhancement, in two ways. The first one is to study the enhancements for different collision energies per incoming nucleon. NA57 has therefore collected data at both 160 and 40 A GeV/c, while WA97 collected data at 160 A GeV/c only. The other one is to study the enhancements for different interaction volumes, measured by the number of wounded nucleons (N_{wound}), i.e. the nucleons which undergo at least one primary inelastic collision with another nucleon [3]. The NA57 centrality range has a lower limit of about 50 wounded nucleons, while the corresponding limit in WA97 was about 100 wounded nucleons.

In this paper, we briefly describe the experiment and we report on the status of the event reconstruction and the physics analysis. We cannot yet compare enhancements at 40 and 160 A GeV/c, since we have not yet analysed the p-Be reference data at 40 A GeV/c collected in August 2001. The main focus of this paper is on checks of the NA57 analysis chain.

2. The NA57 experiment

The NA57 experimental layout [5, 6] is shown in figure 1. The main tracking device is a telescope made of planes of silicon pixel detectors, each plane having a sensitive area of about 5×5 cm^2. The detectors are placed in a 1.5 T vertical magnetic field. The telescope is inclined with respect to the beam line and points back to the target. The hyperons are identified in the telescope through their weak decays into charged particles, e.g.

$$\Xi^- \rightarrow \Lambda + \pi^-$$
$$\quad\quad \hookrightarrow \mathrm{p} + \pi^-$$

The acceptance windows of NA57 are similar to those of WA97, covering about one unit of central rapidity, and transverse momenta down to a few hundred MeV/c [6].

The Pb+Pb sample was collected using a centrality trigger, based on the information from a set of scintillator detectors (Petals) placed 10 cm downstream of the target, which measure the charged particle multiplicity in the pseudorapidity interval $1 < \eta < 2$. The trigger selects the most central 60% of the inelastic cross section. More precise centrality information, used for off-line analysis, is provided by two planes of silicon microstrip detectors (MSD), which sample the charged particle multiplicity in the pseudorapidity interval $2 < \eta < 4$.

The main changes in the NA57 spectrometer with respect to WA97 are:

- a new beam line with a smaller spot size than in WA97, both in the vertical and horizontal directions. Special care was taken in the layout of the beam line in order to keep interactions outside the target to a minimum. This allows for an extended centrality range.
- a different magnet: NA57 uses the GOLIATH magnet, which provides a slightly weaker and less uniform field than the OMEGA magnet used by WA97 (due to the decommissioning of the OMEGA spectrometer in 1997).
- a new telescope layout: only pixels are used for track reconstruction, while WA97 used both pixel and silicon microstrip planes.
- a new data acquisition system [7], and a new data format.

NA57 has collected Pb-Pb data at both 40 and 160 A GeV/c beam momentum, together with a sample of p-Be reference data at 40 GeV/c. For proton reference data at 160 GeV/c, we intend to use the WA97 p-Be and p-Pb data samples.

3. Results from 40 A GeV/c data

The observation of significantly lower enhancements at 40 A GeV/c than at 160 A GeV/c would suggest the onset of a deconfined state to be between these two energies. For such a comparison, p-Be reference data are indispensable. The existing p-Be data are statistically sufficient as reference only for Λ and $\overline{\Lambda}$. A new sample, collected in

	Pb-Pb		p-Be	
	40 A GeV/c	160 A GeV/c	40 A GeV/c	160 A GeV/c
$\overline{\Lambda}/\Lambda$	$\mathbf{0.023 \pm 0.001}$	*0.133 ± 0.007*	$\mathbf{0.059 \pm 0.007}$	*0.332 ± 0.008*
$\overline{\Xi}^+/\Xi^-$	$\mathbf{0.080 \pm 0.025}$	*0.249 ± 0.019*	——	*0.45 ± 0.07*

Table 1. $\overline{\Lambda}/\Lambda$ and $\overline{\Xi}^+/\Xi^-$ ratios. Values from NA57, shown in bold, are not corrected for acceptance and efficiency. Values from WA97 are shown in italics.

2001 and now being processed, should provide an adequate reference also for Ξ^- and $\overline{\Xi}^+$. The complete Pb-Pb sample at this energy has been fully processed, and Λ, $\overline{\Lambda}$, Ξ^- and $\overline{\Xi}^+$ signals are shown in [4].

Table 1 shows the $\overline{\Lambda}/\Lambda$ and $\overline{\Xi}^+/\Xi^-$ ratios measured in Pb-Pb collisions at 40 A GeV/c compared to the published WA97 values [8] at 160 A GeV/c. Also shown are the $\overline{\Lambda}/\Lambda$ ratios for p-Be collisions at both energies. The ratios measured by NA57 (in bold in table 1) have not been corrected for acceptance and efficiency. However, we know that these corrections are small due to the symmetry of our apparatus.

We note that the $\overline{\Lambda}/\Lambda$ and $\overline{\Xi}^+/\Xi^-$ ratios in Pb-Pb collisions decrease by about a factor six and three respectively, when comparing 40 A GeV/c to 160 A GeV/c results. Such a behaviour can be either due to an increase in the baryon density in the initial fireball at lower beam momenta, or simply to a decrease of production cross-sections with beam energy, which is faster for antihyperons than for hyperons, as suggested by the similar behaviour for the $\overline{\Lambda}/\Lambda$ ratio both for Pb-Pb and p-Be collisions.

4. Ξ results from 160 A GeV/c data

In this section we present results from the analysis of Pb-Pb data collected in 1998 at 160 A GeV/c beam momentum. This statistics will be doubled when data collected in 2000 are fully analysed.

We use the number of wounded nucleons, i.e. the nucleons which take part in the initial collisions [3], as a centrality measure. The method used for calculating the number of wounded nucleons is described in [9].

The multiplicity distribution is divided into five centrality classes where the four most central classes correspond to the four classes used by WA97 (class I to IV), while the most peripheral class 0, corresponding to an average of about 62 wounded nucleons, is accessible to NA57 only.

In order to correct for acceptance and efficiency losses, a weight is calculated for each particle [10]. For Ξ^-, $\overline{\Xi}^+$, Λ and $\overline{\Lambda}$, the statistics is large enough to study the centrality dependence down to about fifty wounded nucleons. To do the same for the Ω^- and $\overline{\Omega}^+$, we need the full 1998+2000 data sample. We have chosen to start the computer intensive weighting with the Ξ^- and $\overline{\Xi}^+$ since they are potentially more interesting than Λ and $\overline{\Lambda}$ because of their larger enhancements. Preliminary results on Λ and $\overline{\Lambda}$ are also shown.

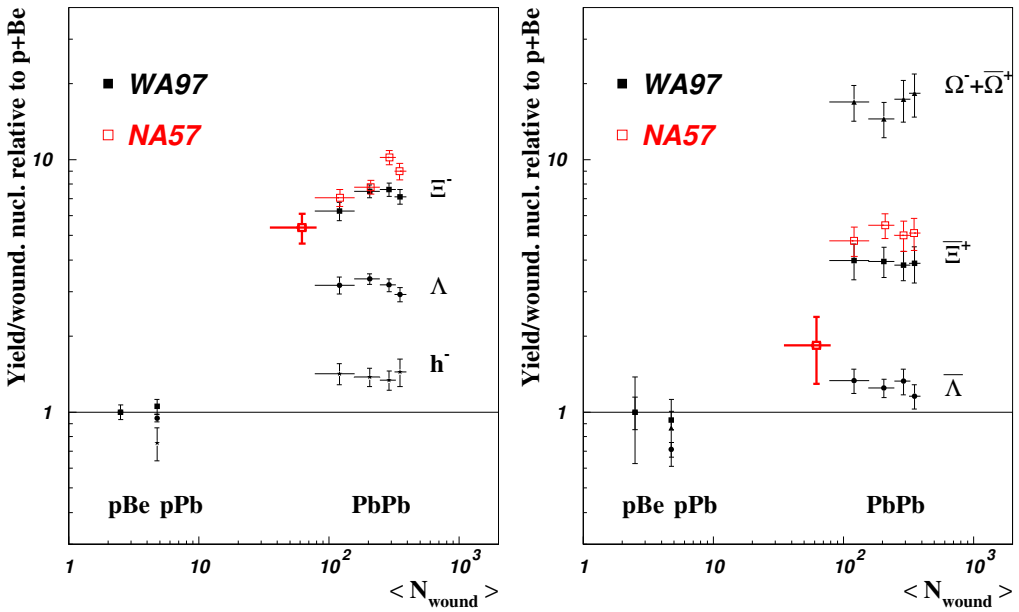

Figure 2. Yields per wounded nucleon relative to the p-Be yields as a function of the number of wounded nucleons, for negative particles, Λ and Ξ^- (left) and for $\overline{\Lambda}$, $\overline{\Xi}^+$ and $\Omega^- + \overline{\Omega}^+$ (right). The NA57 Ξ^- and $\overline{\Xi}^+$ yields (open symbols) are shown together with the WA97 results (closed symbols).

Figure 2 shows the fully corrected particle yields per participant for all the five centrality classes in NA57. The WA97 results (four centrality classes) are also presented. All yields are shown relative to the WA97 p-Be data. The vertical bars indicate the statistical errors. The horizontal line represents the predicted centrality dependence if the yields were to increase proportionally to the number of wounded nucleons all the way from p-Be to central Pb-Pb collisions. We define the enhancement as the deviation from this scaling, i.e. the ratio between the yields per wounded nucleon in Pb-Pb and p-Be collisions. All particle yields are enhanced in Pb-Pb collisions and the enhancement grows with the strangeness content of the hadron, up to a factor of about 15 for the $\Omega^- + \overline{\Omega}^+$. The $\overline{\Xi}^+$ yield per wounded nucleon drops by a factor 2.6 in the most peripheral collisions (class 0). The enhancement seems to be saturated above a mean number of wounded nucleons of about 100. For the Ξ^- the yield drops by a factor 1.3 in the most peripheral collisions. The centrality dependence of the Ξ^- looks different from the one of the $\overline{\Xi}^+$, as the Ξ^- enhancement grows smoothly as a function of the number of wounded nucleons. We note that in the common centrality range, the yields from NA57 are 20-30% larger than the corresponding yields from WA97.

5. Investigation of differences between WA97 and NA57 results

A number of tests of the analysis programs used by WA97 and NA57 have been done. We have tested the methods used in the analysis and in the correction procedure, the

stability of our analysis, and the software. All tests referred to here are done for Ξ^- and $\overline{\Xi}^+$.

The knowledge of the position of the interaction vertex is used for various kinematic cuts in the analysis. There is a difference in the methods used by the two experiments for determining this position. In WA97 the primary vertex position is determined event by event by extrapolating the reconstructed tracks to the target plane. The algorithm of finding a primary vertex for each event becomes inefficient in the new centrality range covered by NA57, where the track multiplicity is very low. In NA57 the beam profile —its average position and spread— has been measured for each run (about half an hour of data taking) using high multiplicity events. The average position and spread are used in the Monte Carlo. This method is possible because of the narrow spot definition (350×650 μm^2 in the directions perpendicular to the beam axis) of the beam and the stability of this position in NA57. In the WA97 correction chain the finite width of the beam spot was neglected in the Monte Carlo. As a result, the correction factors in WA97 are underestimated, and the Pb-Pb particle yields are systematically shifted down by about 10%. The effect shows no multiplicity dependence. This problem does not affect the p-Be results, since a completely different method was used in the analysis of the WA97 p-Be data, where the position of the beam was reconstructed using a beam telescope [11].

In order to check the stability of our analysis, the NA57 Ξ^- and $\overline{\Xi}^+$ yields have been recalculated and corrected for acceptance and efficiency, using different selection criteria. No significant changes in the NA57 results are seen.

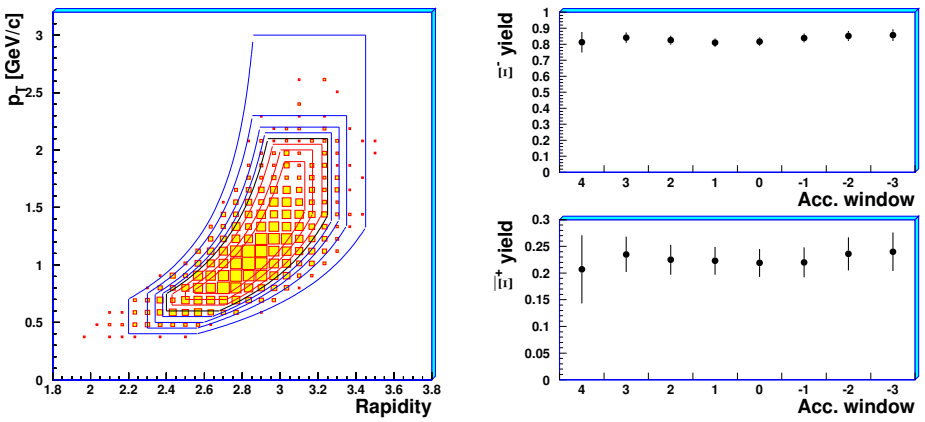

Figure 3. Ξ^- and $\overline{\Xi}^+$ yields (right) for different acceptance windows (left). *Acc.window* = 0 corresponds to our selected window, while *Acc.window* > 0 corresponds to a larger window and *Acc.window* < 0 corresponds to a smaller window.

The Ξ^- and $\overline{\Xi}^+$ yields have also been studied in different time periods, for different magnetic field polarities, and in different acceptance windows (see figure 3) without observing any systematic shift in the final results.

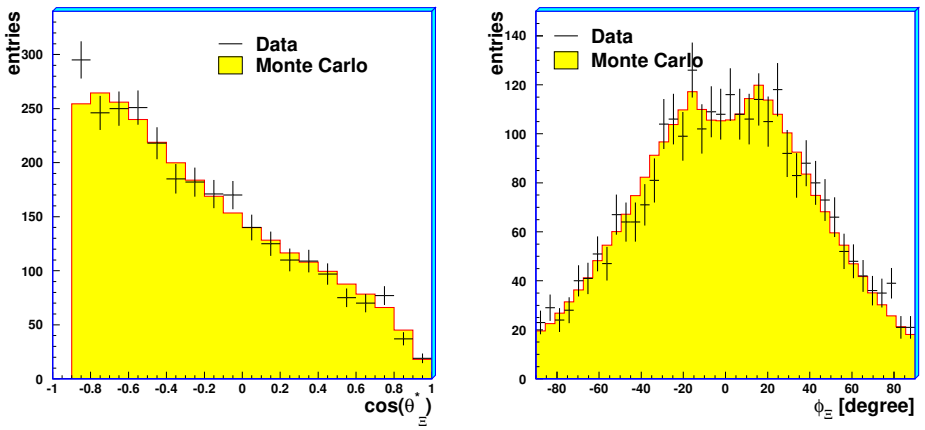

Figure 4. Comparison between real data and Monte Carlo simulations for the internal decay angles in the Ξ reference system, $cos(\theta^*)$ (left) and ϕ (right).

To check the program chain used for calculating correction factors, the Ξ^-s and $\overline{\Xi}^+$s identified in WA97 have been weighted using the NA57 chain of programs. The result is, within statistical uncertainties, the same as the previous WA97 result.

In addition a number of checks have been done to make sure that the simulation used for calculating the correction factors in NA57, reproduces the real data. Some of the comparisons done between simulated and real data are:

- the decay length of the Ξ
- the decay length of the Λ
- the closest distance in space between the extrapolated π and proton tracks coming from the Λ decay
- the π impact parameter§
- the Λ impact parameter with respect to the decay vertex of the Ξ
- the internal decay angles in the Ξ reference system: $cos(\theta^*)$, where θ^* is the angle between the Λ and the Ξ lines of flight in the Ξ reference system, and ϕ is the azimuthal angle (see figure 4).

All tests show agreement between simulated and real data. Finally, using an event mixing method‖, we succeeded in reproducing the observed background in the Ξ^- and $\overline{\Xi}^+$ mass plots.

The outcome of these studies gives us confidence in the NA57 results. We attribute the remaining small differences with respect to the previous experiment WA97 to the improved experimental conditions of the present experiment.

§ The impact parameter is defined as the distance (perpendicular to the beam direction) between the extrapolated lines of flight of the decay particles and the primary vertex.
‖ Study completed after the oral presentation of the paper.

	NA57 class I-IV	WA97 class I-IV	Difference NA57 - WA97
$\overline{\Lambda}/\Lambda$	0.146 ± 0.005	0.133 ± 0.007	0.013 ± 0.009
$\overline{\Xi}^+/\Xi^-$	0.275 ± 0.020	0.249 ± 0.019	0.026 ± 0.028
Ξ^-/Λ	0.105 ± 0.005	0.100 ± 0.004	0.005 ± 0.006
$\overline{\Xi}^+/\overline{\Lambda}$	0.199 ± 0.013	0.188 ± 0.016	0.011 ± 0.021

Table 2. Particle ratios for Pb-Pb data at 160 A GeV/c. The NA57 ratios are preliminary, since the background is still to be subtracted.

6. Λ signals from 160 A GeV/c data

The results presented here are based on Pb-Pb data at 160 A GeV/c beam momentum, collected in 1998. In table 2 preliminary particle ratios for $\overline{\Lambda}/\Lambda$, $\overline{\Xi}^+/\Xi^-$, Ξ^-/Λ and $\overline{\Xi}^+/\overline{\Lambda}$ are presented. The ratios are corrected for acceptance and efficiency, but no background subtraction is done. These preliminary ratios are compatible to the WA97 ratios. The final background subtraction using event mixing is still to be done before the fully corrected Λ and $\overline{\Lambda}$ yields can be presented.

7. Conclusions

Some discrepancy between WA97 and NA57 was reported at the Quark Matter 2001 conference [4]. Since then we have proceeded to thorough checks of the NA57 analysis chain. The outcome gives us confidence in the NA57 results. A part of the discrepancy has been accounted for. Remaining differences are attributed to the improved experimental conditions in NA57. Both the Ξ^- and $\overline{\Xi}^+$ yields for Pb-Pb collisions at 160 A GeV/c drop significantly in the most peripheral centrality class, by factors of 1.3 and 2.6 respectively. The drop in the $\overline{\Xi}^+$ yield per wounded nucleon might indicate the onset of the QGP phase transition.

References

[1] Fini R A *et al* 2001 *J. Phys. G: Nucl. Part. Phys.* **27** 375
Antinori F *et al* 1999 *Nucl. Phys.* **A661** 130c
[2] Rafelski J and Müller B 1982 *Phys. Rev. Lett.* **48** 1066
[3] Wong C Y 1994 *Introduction to High-Energy Heavy-Ion Collisions* (World Scientific Publishing, Singapore) p 251, and references therein
[4] Carrer N *et al* 2002 *Nucl. Phys.* **A698** 118c
[5] Manzari V *et al* 2001 *J. Phys. G: Nucl. Part. Phys.* **27** 383
[6] Manzari V *et al* 1999 *Nucl. Phys.* **A661** 716c
[7] Vande Vyvre P *et al ALICE Internal Note/DAQ* **99/46**
[8] Caliandro R *et al* 1999 *J. Phys. G: Nucl. Part. Phys.* **25** 171
[9] Carrer N *et al* 2001 *J. Phys. G: Nucl. Part. Phys.* **27** 391
[10] Antinori F *et al* 2000 *Eur. Phys. J.* **C 14** 633
[11] Elia D *et al* 1999 *Nucl. Phys.* **A661** 476c